atmosphere

MDPI

Review

Seasonal Variations and Sources of 17 Aerosol Metal Elements in Suburban Nanjing, China

Lu Qi [1,2,3], Mindong Chen [1,2,3,*], Xinlei Ge [1,2,3,*], Yafei Zhang [1,2,3] and Bingfang Guo [1,2,3]

1 Collaborative Innovation Center of Atmospheric Environment and Equipment Technology, Nanjing 210044, China; lu.qi@psi.ch (L.Q.); yafeizhang1@gmail.com (Y.Z.); bingfangg@gmail.com (B.G.)
2 Jiangsu Key Laboratory of Atmospheric Environment Monitoring and Pollution Control, Nanjing 210044, China
3 School of Environmental Science and Engineering, Nanjing University of Information Science & Technology, Nanjing 210044, China
* Correspondence: chenmd@nuist.cn (M.C.); caxinre@gmail.com (X.G.)

Academic Editor: Robert W. Talbot
Received: 16 October 2016; Accepted: 22 November 2016; Published: 25 November 2016

Abstract: In this work, the seasonal variations and sources of trace metal elements in atmospheric fine aerosols ($PM_{2.5}$) were investigated for a year-long field campaign from July 2012 to June 2013, conducted in suburban Nanjing, eastern China, at a site adjacent to an industry zone. The $PM_{2.5}$ samples collected across four seasons were analyzed for 17 metal elements, namely, Sodium (Na), Magnesium (Mg), Aluminum (Al), Vanadium (V), Chromium (Cr), Manganese (Mn), Nickel (Ni), Copper (Cu), Zinc (Zn), Arsenic (As), Selenium (Se), Strontium (Sr), Cadmium (Cd), Barium (Ba), Lead (Pb), Molybdenum (Mo), and Antimony (Sb) using an inductively coupled plasma mass spectrometry (ICP-MS). We found that the total concentration of all 17 metal elements was 1.23 $\mu g/m^3$, on average accounting for 1.0% of the total $PM_{2.5}$ mass. For our data, mass concentrations of Al, Cd, Ba were highest in summer, Mg, Cu, Zn, Se, Pb peaked in autumn, Cr, Mn, Ni, As, Sr, Sb increased significantly in winter, while the concentrations of Na, V, Mo were at their highest levels in spring. Air mass back trajectory analysis suggested that air parcels that arrived at the site originated from four dominant regions (Japan, yellow sea and bohai; Southeast of China, the Pacific Ocean; Southwest of Jiangsu and Anhui province; Northern Asia inland and Mongolia region), in particular, the one from Northern Asia inland and Mongolia contained the highest concentrations of As, Sb, Sr, and was predominant in winter. Positive matrix factorization (PMF) analyses revealed that the industrial emission is the largest contributor (34%) of the observed metal elements, followed by traffic (25%), soil dust (19%), coal combustion (10%), incineration of electronic waste (9%), and a minor unknown source (3%). In addition, we have also investigated the morphology and composition of particles by using the scanning electron microscopy (SEM)/energy-dispersive spectrometry (EDS) techniques, and identified particles from coal burning sources, etc., similar to the PMF results.

Keywords: metal elements; aerosol; seasonal variations; source apportionment

1. Introduction

Ambient particulate matter (PM) pollution, is emerging as one of the leading risk factors of mortality, ranking in the sixth place in 2010 [1,2] from the 13th place in 2000 among all risk factors [3]. Atmospheric PM came not only from natural sources, including volcanic eruptions, crustal materials, surface dust, sea spray, wildfires, etc., but also from a variety of anthropogenic sources such as coal combustion, vehicular emissions, biomass burning and industrial emissions, and so on [4–8]. Various metal elements are ubiquitous constituents of ambient PM, and most of them are chemically stable, thus the transport and dispersion of atmospheric aerosol particles can largely expand their

influences [6,9,10]. For instance, as atmospheric fine particles can travel over a long distance downwind from the sources [11–13], the airborne metallic species can affect the terrestrial and aquatic ecosystems, at both regional and global scales via dry and wet depositions [14–19]. Inhalation of the airborne metallic species is also detrimental to human health. Hence, a detailed elucidation of the temporal variations and sources of trace metals is of central importance to evaluate their environmental and health consequences [20,21].

Monitoring networks for PM-metal elements have already been established at urban, suburban, rural, mountain, forest, industrial sites, or near heavy traffic roads in many countries including America [22,23], India, United Kingdom [24] and other European countries [25–27]. Previous studies that focused on the distribution of metal elements in different sizes of aerosol particles [9,28–30] found that elements such as aluminum, iron, strontium, zinc mainly existed in coarse particles, whereas vanadium, nickel, lead, cadmium mostly resided in fine particles [31,32]. Sources of metal elements have been investigated by methods including Enrichment Factors (EF), Principal Component Analysis (PCA) and Positive Matrix Factorization (PMF), etc., and typical sources identified include coal combustion, vehicle emission, mineral dust and so on [13,33–35]. The connections between atmospheric deposition of metal elements and contamination of soil and bryophyte have also been investigated [12,36]. Furthermore, the bioavailability, health risk evaluation, and epidemiological inter-disciplinary studies of metal elements were also reported previously [2,37,38].

Recently, air pollution has become a serious and pressing issue along with the fast economic development in China. However, the airborne heavy metal pollution still remains not fully understood, in particular, the detailed emission inventories due to the fact that the corresponding monitoring system has not been set up [37,39]. Moreover, many studies that focused on analysis of the concentrations and size distributions of metal elements were conducted in a few major heavily polluted megacities such as Beijing, Shanghai and Guangzhou, and covered relatively short time periods [40–45]. Nanjing, as the second largest city in the Yangtze River Delta region in Eastern China, with a river shoreline of about 2 hundred kilometers, an area of 752.83 square kilometers and a population of 8.19 million, also suffered serious air pollution in the past decades due to increasing emissions from traffic (gasoline and diesel combustions, tire and brake lining wear, etc.), industry (petrochemical activities), coal burning, and so on [29,46]. However, studies regarding the temporal, seasonal variations and source contributions of atmospheric metal elements in Nanjing are very scarce.

Previously, we have investigated the mass loadings and sources of 15 trace metals in the $PM_{2.5}$ samples during the second Asian Youth Games period in urban Nanjing [47]. Here, we further performed analyses of 17 metal elements in $PM_{2.5}$ samples collected near one-year period from 28 July 2012 to 31 June 2013 in suburban Nanjing. The metal elements analyzed include sodium (Na), magnesium (Mg), aluminum (Al), vanadium (V), chromium (Cr), manganese (Mn), nickel (Ni), copper (Cu), zinc (Zn), arsenic (As), selenium (Se), strontium (Sr), cadmium (Cd), barium (Ba), lead (Pb), molybdenum (Mo) and antimony (Sb). In this work, we aim to: (1) determine the mass concentrations of 17 metal elements, and their contributions to the total $PM_{2.5}$ mass loading; (2) investigate the seasonal variations by combining with the meteorological parameters; and (3) identify the major sources of aerosol metal elements in this region using PMF model. Our results are valuable for the implementation of appropriate measures to reduce the atmospheric metal and $PM_{2.5}$ pollution in this region.

2. Methodology

2.1. Site Description

The sampling site is located at the campus of Nanjing University of Information Science and Technology in suburban Nanjing (32.21°N, 118.72°E), in the provincial capital of Jiangsu Province, as shown in Figure 1. The site is east of a rural field, and east/northeast of an industry zone with a large number of factories including iron and steel making plants, petrochemical and chemical engineering

factories, and electronic plants, etc. The site is also influenced by other human activities, such as traffic, cooking, and biomass (straw and crop) burning, etc.

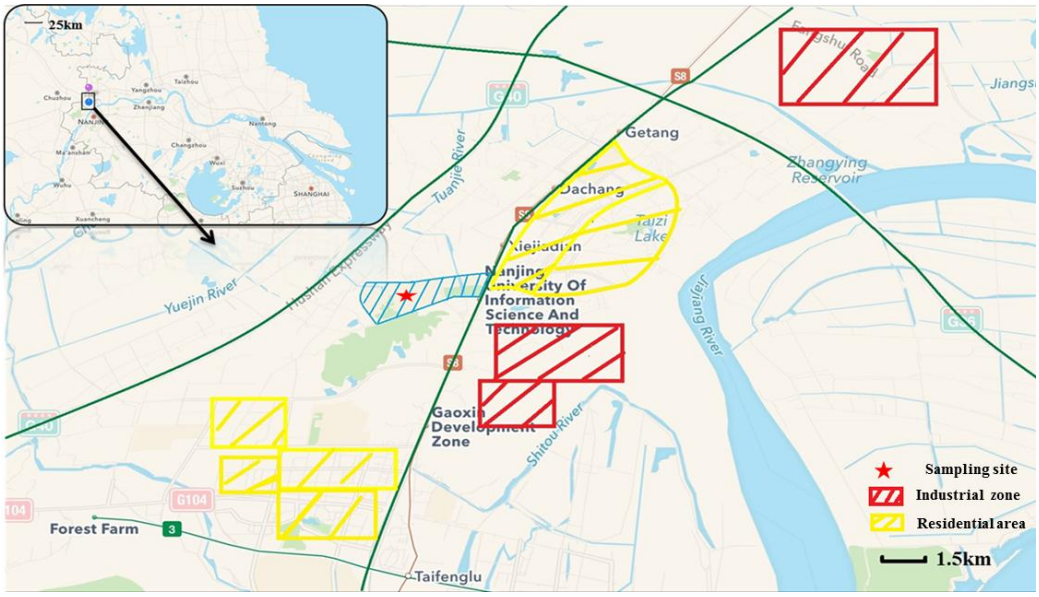

Figure 1. Location of sampling site in Nanjing, Jiangsu Province, the eastern China.

During the sampling period, meteorological parameters (air temperature, relative humidity, wind speed, wind direction) were recorded (Figure 2) at the meteorological station located at the same site.

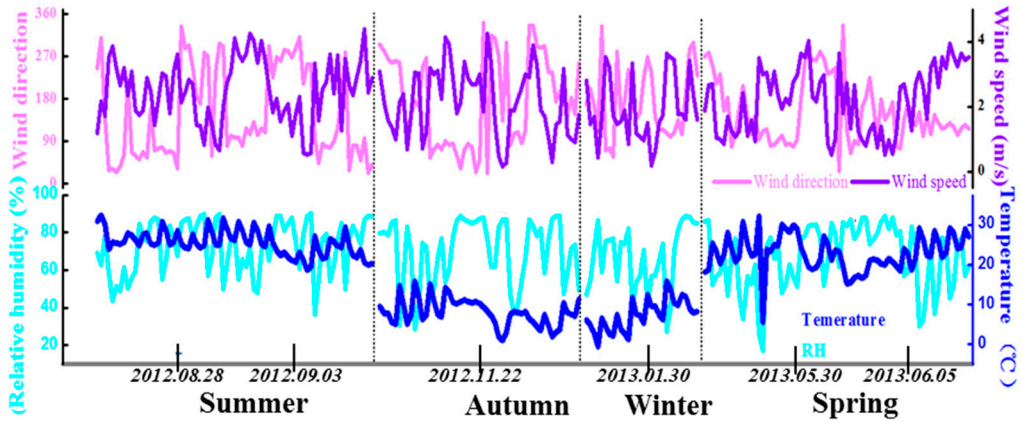

Figure 2. Temporal variations of meteorological parameters from 2012 to 2013 during the sampling campaign.

2.2. Sample Collection and Preparation

The $PM_{2.5}$ samples were collected in four seasons, including Summer (23 August–8 September 2012), Autumn (17–28 November 2012), Winter (25–30 January 2013), and Spring (20 May–6 June 2013). Note that although we only collected samples for a limited number of days in each season, the sampling days and results should be representative of the corresponding seasons—as shown clearly in Figures S1–S5 in the supplement, the meteorological parameters, including wind speed, wind direction, temperature and RH, averaged over the sampling days are very similar to the corresponding seasonal average values. In total, 64 $PM_{2.5}$ samples (details in Table S1) were collected on the Whatman mixed cellulose ester filters (GE healthcare UK limited, Amersham place, Little Chalfont, England) in summer,

autumn, spring and on the Whatman quartz fiber filters in winter (9 cm diameter) using a median volume atmospheric particle sampler (HY-100, Qingdao Henyuan Instruments Co. Ltd., Qingdao, China) equipped with a $PM_{2.5}$ cyclone. The flow rate was 100 L·min^{-1}, and was calibrated every day during sampling.

All filters before sampling were firstly baked in a muffle furnace (450 °C) for four hours, wrapped in tinfoil and put into a constant temperature (at 25 °C) and relative humidity (50%) chamber for 48 h, and then were weighed. The sampling time for each sample was 12 h (we did not observe significant differences between daytime and nighttime samples as the sampling time resolution is low and metals are relatively stable, we reported results below without daytime-nighttime comparisons). Sampling was not conducted at rainy and snowy days as wet deposition can efficiently scavenge the atmospheric pollutants and high air relative humility may damage the filters. After sampling, the filters were equilibrated in the constant temperature and relative humidity chamber for 48 h, weighed, placed individually inside zip-sealed bags, and were then stored in the refrigerator at −4 °C in laboratory prior to analysis. Note Illuminati et al. [48] provided a very strict, precise aerosol mass measurement procedure with careful decontamination step, and filter blanks were also treated with more accuracy test—to ensure the accuracy of the measured aerosol mass concentrations. These procedures will be applied to our future studies if possible.

2.3. Sample Analyses

For the measurement of metal elements in environmental samples such as aerosol particles, soil, and municipal water, microwave digestion has recently been widely employed for sample pretreatment [47,49–51]. In this study, a MARS6 Xpress CEM corporation Microwave Digestion System was used to digest the $PM_{2.5}$ constituents. About 1/8 of a filter was weighed, cut into pieces and put into the PTFE pressure digestion tank, and then dissolved in 5 mL 69% nitric acid (HNO_3) and 1 mL 49% hydrofluoric acid (HF). The digestion tanks (16 samples in a batch) were sealed and processed according to the programmed procedure consisted of three steps: (1) raise the temperature to 190 °C in 20 min; (2) maintain the temperature at 190 °C for 25 min to achieve a complete digestion; (3) cool down to room temperature in about 30 min. The digested solutions were then transferred into a vacuum filtration system, to remove the excess HF and HNO_3 solutions, and then diluted to 45 mL with purified water in a 45 mL centrifuge tube kept at 4 °C. In addition, blank filters were treated in the same way. All sample containers are made of polypropylene, high-density polyethylene Teflon to minimize possible contaminations.

The concentrations of 17 metal elements in the solutions were analyzed using an Thermo Fisher X2 Series Inductively Coupled Plasma Mass Spectrometry (ICP-MS), which has an ICP source, Optimization system (extracting and focusing of the ion beam), a quadrupole mass spectrometer and a detector. The instrument has high mass sensitivity and selectivity, and was calibrated daily according to the standard protocol provided by the manufacturer. External multi-element standard solution (XCCC-13A, XCCC-14B, SPEX CertiPrep Group, Metuchen, NJ, USA) was used to establish a four-points (2 ppb, 5 ppb, 10 ppb, 18 ppb) standard curve, and internal standard, which was 2 ppb ^{45}Sc, ^{115}In mixed solution (60201SS, Inorganic Ventures Corporation, Christiansburg, VA, USA) was used to eliminate the interferences of other elements to the targeted elements.

2.4. Quality Assurance and Quality Control

Quality assurance and quality control procedures were applied during sampling, handling and measurement steps, in order to minimize possible artifacts. Two certified materials of soil (GBW07403) and fly ash (GBW08401) were measured in parallel to ensure high quality. NIST 1648 and 1648a as pointed by Illuminati et al. [49] can also be used as urban particulate reference material to check the accuracy of the measurements, which should be investigated further in the future. Nevertheless, under the current digestion and the analysis procedures mentioned above, all elements are within the

target recovery of 100% ± 15%. Four levels of calibration standards were used, and the correlation coefficients of standard curves were all greater than 0.999.

In this work, the limit of detection (LOD) of each element was calculated according to ICH Q2B (ICH 2005) using the following equations [52]:

$$\text{LOD} = 3.3\ \text{Sa/b}$$

where Sa = standard deviation of the intercept of regression line and b = slope of the calibration curve [53,54]. The LOD in air was calculated by the formula: LOD in air (ng·m^{-3}) = concentrations in solution (μg·L^{-1}) × 0.045 L/72 m^{-3}. By using this approach, the LODs of Na, Mg, Al, V, Cr, Mn, Ni, Cu, Zn, As, Se, Sr, Cd, Ba, Pb, Mo, and Sb were determined to be 2.36, 0.98, 1.20, 0.17, 1.09, 0.88, 1.19, 1.08, 1.15, 0.92, 0.54, 0.98, 1.14, 0.27, 0.95, 0.19 and 0.25 ng·m^{-3}, respectively. The average concentrations of all 17 elements in the $PM_{2.5}$ samples were higher than the LODs. The blank filters were treated in the same way as for the samples, and the mean values of Na, Mg, Al, V, Cr, Mn, Ni, Cu, Zn, As, Se, Sr, Cd, Ba, Pb, Mo, Sb in blank filter of mixed cellulose ester were 34, 11.4, 16.8, 0.15, 1.2, 0.55, 0.3, 0.12, 1.57, 0.85, 0.11, 0.03, 0.08, 0.25, 0.06, 0.19, 9.2 ng·m^{-3}, respectively; the background data of quartz fiber filter were 22.31, 8.55, 3.75, 0.08, 0.33, 0.14, 0.78, 0.85, 4.88, 0.19, 0.12, 0.27, 0.01, 0.3, 0.07, 0.05, 5.6, 9.2 ng·m^{-3}, respectively. These background values were well below the corresponding values in the filter samples, indicating that filter itself did not interfere the observed concentrations significantly. All results reported in this study were subjected to blank filter correction.

2.5. Scanning Electron Microscopy

Particle morphology of aerosol samples was investigated by using the scanning electron microscopy (SEM) (S-3400N II, Hitachi High. Technologies Corporation, Tokyo, Japan). The SEM technique can show the detailed morphology of a single aerosol particle. The samples were analyzed by cutting 1 cm^2 of the filter, and mounted onto an Al stub, coated by gold nanoparticles, and then placed into the instrument operated with a resolution at 20 kv, 1280 × 960 pixel. Compositions of the SEM-imaged particles were also analyzed by the Energy Dispersive Spectrometer (EDS) (Hitachi, Tokyo, Japan).

2.6. PMF Analysis

Positive matrix factorization (PMF) [55,56] is a multivariate factor analysis model recommended by the EPA. A unique advantage of the PMF algorithm is that the model considers the measurement uncertainties corresponding to the observed data to weigh the data points, and thus output the source profiles that can well represent the real characteristics. Of course, Principal Component Analysis (PCA) related methods (e.g., Padoan et al. [57]) are also useful for the source apportionment analyses. In this study, we used EPA (Environmental Protection Agency) PMF 3.0 to identify and apportion possible sources to the observed metal elements. The data matrix X of the samples can be represented as the product of two matrices (the concentration series of G and the factor profiles F) plus a residual matrix E that accounts for the unexplained portion of the measured data [46].

$$x_{ij} = \sum_{k=1}^{p} g_{ik} f_{kj} + e_{ij} \quad (i = 1, \ldots, n;\ j = 1, \ldots, m;\ k = 1, \ldots, p)$$

$$Q = \sum_{i=1}^{n} \sum_{j=1}^{m} \left[\frac{e_{ij}}{u_{ij}} \right]^2$$

Supposing matrix X is $n \times m$ (n rows are concentration series of the samples; m columns are the elements determined), G is the $n \times p$ matrix (p, numbers of possible sources) and F is a $p \times m$ matrix. u_{ij} is the estimated error (standard deviation) of the corresponding data points in the matrix X. One constraint of PMF model is that the data of metal elements are all non-negative. Both the data and error matrices were pre-processed following the protocols detailed in the EPA PMF user manual. The PMF algorithm was run in robust mode, and a few outliers were excluded during calculations, in order to eliminate unreasonable influences of these data on the PMF results.

3. Results and Discussion

3.1. Characteristics of Metal Elements

3.1.1. Annual Characteristic of Metal Elements

The measured mass concentrations (minimum, maximum, mean, median, standard deviation, skewness and kurtosis) of the 17 metal elements and $PM_{2.5}$ were summarized in Table 1. Concentrations of four elements, e.g., Al, Cu, Mo, Sb, varied dramatically in 2 orders of magnitude in different days, while variations of other elements were on one order of magnitude. The skewness coefficients of 13 elements were within 0~2, indicating that there is little right-skewed distribution in the samples; hence the median values were typically lower than the mean values except for Al. Most of the kurtosis coefficients were larger than zero. This result demonstrates that concentration distribution of samples was narrower and steeper than the normal distribution, especially for the elements featured with relatively high concentrations, such as Al (10.31), Cu (22.2), Zn (11.8) and Mo (11.55), likely indicating emission sources of soil dust, traffic and Mo source (detailed in Section 3.2) in suburban Nanjing.

Table 1. Concentrations of $PM_{2.5}$ metal elements in suburban Nanjing during 2012–2013 (ng/m^3).

	Min	Max	Mean	Medium	SD	Skewness	Kurtosis
$PM_{2.5}/10^4$	4.56	40.30	12.50	17.50	6.42	1.59	-
Na	170.53	777.89	369.10	355.71	122.17	1.02	1.23
Mg	137.89	453.72	246.40	243.28	67.85	0.59	0.42
Al	2.96	607.16	114.95	127.71	95.92	2.22	10.31
V	0.84	8.82	3.95	3.81	1.81	0.55	−0.07
Cr	5.61	54.63	24.76	19.60	15.48	0.28	−1.51
Mn	17.00	153.54	58.97	56.02	30.05	0.62	0.32
Ni	3.53	18.89	8.10	7.01	3.53	1.32	1.49
Cu	7.80	206.20	29.44	22.27	29.30	4.17	22.20
Zn	64.87	850.00	254.80	237.98	167.23	2.89	11.80
As	1.47	21.06	6.30	4.06	4.95	1.26	0.62
Se	1.23	8.41	4.51	4.07	1.91	0.50	−0.74
Sr	2.56	15.14	5.99	4.92	2.87	1.10	0.74
Cd	0.46	6.62	2.09	1.72	1.38	1.64	3.19
Ba	7.52	65.57	20.00	16.25	10.44	1.88	4.93
Pb	15.26	145.50	67.37	66.18	25.53	0.36	0.38
Mo	0.96	51.19	8.48	6.74	8.42	3.02	11.55
Sb	0.31	10.14	2.37	1.50	2.30	1.82	3.08
Total metal	571.04	3324.24	1227.58	1178.79	-	-	-

SD: Standard deviation.

The $PM_{2.5}$ mass concentrations ranged from 45 to 403 μg/m^3 with an average mass loading of 125 μg/m^3, and the total concentration of 17 metal elements was 1.227 μg/m^3, accounting for 1.0% of the total $PM_{2.5}$ mass. These findings are similar to a study conducted at Ji'nan industrial and urban sites (130 μg/m^3 of $PM_{2.5}$ mass concentrations and 1.62 μg/m^3 of metals), where ferrous metal smelting, traffic equipment production, and petrol processing are large emitters of metals, in particular Sb, Cd, As, Se [58]. In the samples (Table 1), Na, Mg, Al were the crustal elements, with higher concentrations than other elements except for Zn. Zn was found to be the most abundant heavy metal element, with concentrations ranging from 64.87 to 850 ng/m^3 and an average of 254.80 ng/m^3. Pb and Mn also had relatively high concentrations, on average, of 67.37 ng/m^3 and 58.97 ng/m^3, respectively, following by Cu, Cr, and Ba, all of which varied in a relatively wide range. The concentration of Pb in Nanjing was far below the limits of current National Ambient Air Quality Standard (NAAQS) of China (GB3095-2012) and that of World Health Organization (WHO) of 500 ng/m^3. The average concentrations of Mo, Ni, As, Sr, Se, V, Sb, Cd were all less than 10 ng/m^3. However, the average concentration of As (6.3 ng/m^3) was higher than the NAAQS limit of 6 ng/m^3. Details regarding the sources of metal elements are presented in Section 3.2.

Table 2 compares our results with previous measurements of the metals in $PM_{2.5}$ samples collected from various sites, including rural, urban, industrial, forest, suburban, mountain, and island sites cities in China, Europe and United States [28,31,33,59,60]. Overall, the concentrations of dust-related metal elements in suburban Nanjing were at similar levels compared with those from some rural sites in foreign countries like Switzerland, Los Angles, USA, but with higher concentrations of some heavy metals derived from vehicle and industrial emissions, although levels of these metals appear to be lower than those in a few cities, such as Xi'an, Ji'nan and Zhuzhou [33]. In details, concentrations of Na, Mg, Al measured in this study were much lower than those found at the rural sites of China, while generally higher than the reported concentrations in other countries such as Switzerland [46] and Los Angles, USA [23]. As these three elements are relevant to the soil or dust-derived sources, it is obvious that their concentrations were higher in rural area (Table 2). Concentrations of V, Mn, and Ni were closer to those measured in rural site, lower than in urban locations. The average concentrations of Cu, Se, Cd, As and Sb were higher at urban sites than those at rural sites presumably indicating the significant contributions from local emission sources to these elements in Nanjing. Zn and Pb behaved differently from other elements, which is discussed in detail later.

Overall, our results together with previous observations in Table 2 showed that particle-phase metal concentrations in urban/industrial areas were much higher than those in rural/mountain areas, indicating that anthropogenic emissions such as industrial production contribute significantly to urban atmospheric metals. For example, in industrial areas of Ji'nan [58] or Zhuzhou, China, the metal elements like Mn, Cu, Zn, As, Pb were several orders of magnitude higher than those at mountain or rural sites, such as Mountain XL and rural areas near Beijing [29]. As mentioned earlier, high concentrations of As exceeding the limits of 6 ng/m^3 of the national standard were observed in many cities in China, in particular Hangzhou (120 ng/m^3), Zhengzhou (185.2 ng/m^3) [39], Ji'nan (60 ng/m^3), Shanghai (30.8 ng/m^3), and Zhuzhou (42 ng/m^3).

Table 2. Concentrations of metals in Nanjing $PM_{2.5}$ and aerosol metal concentrations in a selection of previous studies of China and other countries.

	Na	**Mg**	**Al**	**V**	**Cr**	**Mn**	**Ni**	**Cu**	**Zn**	**As**	**Se**	**Sr**	**Cd**	**Ba**	**Pb**	**Mo**	**Sb**
Nanjing	390	255.8	121.3	4.1	28.7	65.5	8.1	32.2	281.9	7.2	4.7	6.2	1.9	18.3	68.2	9.5	2.8
Beijing, China (2011), suburban [35]	1449	637	2182	25	21.8	35.6	20.2	10	27.8	2.9	1.1	9.8	1.1	18.4	52.9	6.5	0.6
Switzerland (2006), rural [46]	298	48	91	0.7	-	2.8	1.2	6	-	0.53	0.16	-	0.32	-	-	-	-
Cordoba, Argentina (2010), rural [23]	1928	-	-	-	-	95.78	5.71	5.55	17.66	1.26	0.36	-	0.8	45.8	4.63	-	-
Los angles, USA (2009), rural [23]	66.5	30.8	107	2.36	1.48	3.76	1.23	8.93	10	0.27	-	1.16	0.09	5.44	2.52	0.45	1.08
Xi'an, China (2012), urban campus [60]	-	-	-	68	145.4	538.9	31.2	57.4	319.5	10.2	-	-	-	914.6	131.8	-	-
Ji'nan, China (2010), industrial [58]	-	-	670	-	10	110	10	40	440	60	-	10	-	20	200	-	-
Zhuzhou, China (2012), industrial [33]	-	-	-	-	115	-	35	98	1140	42	-	-	10.3	-	254	-	9.8
Oxford, UK (2007), urban [31]	-	-	-	3.9	1.2	3.5	67.3	39.5	30	-	-	25.4	1.06	-	186	0.4	-
Shanghai, China (2012), urban [39]	-	-	-	10.3	27.3	60.3	10	35.5	418.5	30.8	-	-	2.9	-	108.5	-	-
Mountain XL, China (2012) [29]	888	540	323	18.9	78.6	29.4	12.9	43.7	140	-	5.09	-	11.26	33.3	57.2	1.07	21.3
S-E Finland (2006), forest [28]	-	100	-	2.7	-	7.3	1.3	2.6	20	0.85	-	-	-	-	13	-	-
Venice Lagoon (2002) [59]	370	-	400	12	-	16	14	10	60	3	-	2	2	-	19	-	-
Los angles, USA (2009), urban [23]	41.4	11.8	46.5	3.72	1.22	1.78	1.38	9.02	8.05	0.22	-	0.83	0.06	6.22	1.79	0.44	1.17

3.1.2. Seasonal Variations of Atmospheric Metals

The average seasonal mass concentrations (±SD) of $PM_{2.5}$ and the 17 metal elements are shown in Table 3. Figure 3 shows the time-dependent concentrations of the 17 metal elements during the four seasons. The highest $PM_{2.5}$ levels were found in winter (162 $\mu g/m^3$), followed by autumn (139 $\mu g/m^3$), spring (119 $\mu g/m^3$) and summer (106 $\mu g/m^3$). These values are a few times higher than the $PM_{2.5}$ standards of the Air Quality Guideline of World Health Organization (WHO) (25 $\mu g/m^3$), and also much higher than the Ambient Air Quality Standard set by the Chinese Environmental Protection Bureau (75 $\mu g/m^3$), reflecting the serious air pollution in suburban Nanjing.

Table 3. Seasonal variations of atmospheric $PM_{2.5}$ metals (mean ± SD, ng/m^3) during the study period. (SD: Standard deviation).

	Summer	Autumn	Winter	Spring
$PM_{2.5}/10^4$	8.2	16.9	16.8	11.3
Na	312.73 ± 134.34	307.24 ± 44.63	395.39 ± 77.93	444.79 ± 114.94
Mg	224.21 ± 85.21	271.05 ± 66.55	262.36 ± 55.66	252.37 ± 50.29
Al	140.58 ± 129.15	97.74 ± 71.56	113.2 ± 51.34	87.84 ± 87.42
V	3.48 ± 2.21	3.08 ± 1.27	4.19 ± 0.99	4.77 ± 1.74
Cr	9.84 ± 4.2	39.21 ± 2.22	39.21 ± 6.97	37.81 ± 10.39
Mn	37.97 ± 22.1	66.92 ± 23.46	70.31 ± 23.23	68 ± 33.49
Ni	7.69 ± 3.63	7.82 ± 2.61	8.76 ± 3.26	8.25 ± 4.06
Cu	17.84 ± 9.37	52.65 ± 63.88	34.58 ± 12.08	24.17 ± 11.49
Zn	166.60 ± 68.24	363.48 ± 203.79	309.99 ± 111.10	257.15 ± 212.85
As	2.90 ± 0.92	8.95 ± 6.01	12.1 ± 4.78	4.77 ± 3.1
Se	3.41 ± 1.35	5.62 ± 1.85	5.48 ± 1.73	4.21 ± 1.74
Sr	4.85 ± 2.74	6.51 ± 2.92	7.55 ± 2.41	5.44 ± 2.05
Cd	2.68 ± 1.9	2.26 ± 0.72	2.52 ± 1.06	1.15 ± 0.56
Ba	23.14 ± 14.09	18.26 ± 9.11	23.06 ± 7.12	15.17 ± 6.14
Pb	62.95 ± 31.66	76.61 ± 20.66	72.19 ± 14.46	62.46 ± 24.68
Mo	4.37 ± 3.01	7.31 ± 3.85	10.06 ± 4.1	11.48 ± 12.38
Sb	0.82 ± 0.45	2.61 ± 1.45	5.71 ± 2.64	1.84 ± 1.34
Total	1066.74	1356.79	1421.77	1353.68

For the 17 metal elements, the highest levels of Cr, Mn, Ni, As, Sr and Sb occurred in winter, average concentrations of Mg, Cu, Zn, Se and Pb peaked during autumn, Al reached its maxima in summer, while Na, V, Cd, Ba and Mo were found at high levels during both winter and spring. The variations of concentrations in different seasons can be represented by the standard deviations (SD), as shown in Table 3. Large SD values were mostly found during summer and spring, except for Cu, As, Se, and Sr in autumn, and Mo in winter. The Cr concentrations were elevated significantly during winter and spring, similar to Na; the concentrations of Zn, as well as As, Se, and Sb, also varied dramatically in autumn and winter, (Figure 3). On the contrary, V and Ni showed a similar trend, with low levels observed in autumn and winter and high levels in summer and spring. So the opposite trends from the two groups of metal elements indicate that they may originate from different sources. Both Cd and Ba had maximum values in summer and showed a higher degree of variation in summer. It is worth mentioning that Cu had a unique distribution during four seasons (Figure 3) with the highest concentrations occurring in autumn, but appeared to be relatively flat during other seasons. Source contributions of metal elements varied during different seasons. For example, coal burning is remarkably high in cold seasons (such as winter), so it may emit high amounts of As and Sr, and industrial emissions may contain more V and Ni. The relationship between the sources and seasonal variations of the metals is further discussed in Section 3.2. In addition, it also should be noted that, besides the different emission sources, the average boundary layer heights in different seasons may influence the measurement results as well.

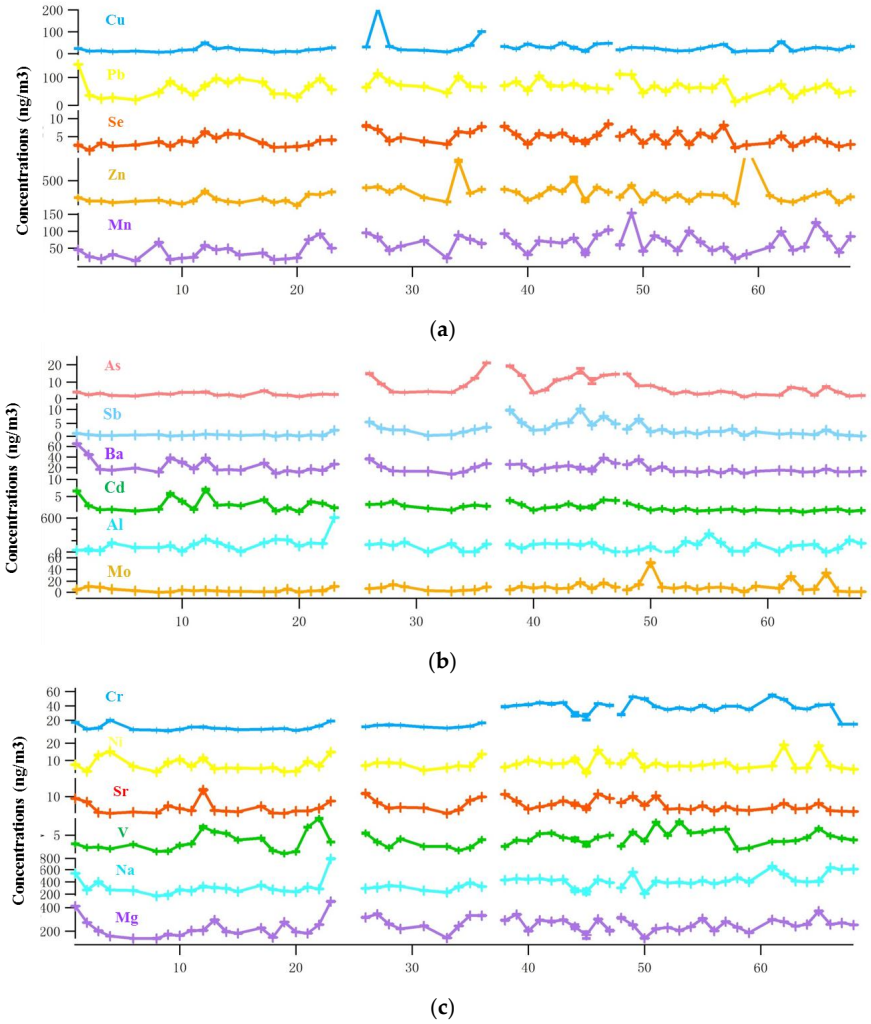

Figure 3. Temporal variations of the 17 metal elements in $PM_{2.5}$. (**a**)Time series of metal Cu, Mn, Pb, Zn, Se; (**b**) Time series of metal As. Sb, Ba, Cd, Al, Mo; (**c**) Time series of metal Cr, Ni, Sr, V, Na, Mg.

3.1.3. Meteorological Influences

The temporal variations of meteorological parameters throughout the campaign are presented in Figure 2. The average temperatures in summer, autumn, winter and spring are 25.4 °C, 8.3 °C, 2.8 °C and 21.5 °C, and average relative humidity are 72.9%, 70.2%, 70.3%, and 64.7%, respectively. In summer, both the air temperature and relative humidity are higher than those in other seasons, which may enhance the secondary formation of other aerosol components, such as sulfate or secondary organic aerosols, altering the $PM_{2.5}$ compositions and thus the fractional contributions of metals. However, on the other hand, high temperature may also lead to the evaporation of semi-volatile species and decrease the $PM_{2.5}$ mass loadings. Overall, the influences of temperature and humidity of the variations and contributions of metals in $PM_{2.5}$ are complex, and should be investigated in the future with other supporting data.

The air mass back trajectories in the four seasons were calculated using the Hybrid Single-Particle Lagrangian Intgrated Trajectory (HYSPLIT) model (Figure 4), based on the meteorological parameters [61,62]. In this study, the air parcels were traced 72 h back in time to estimate trajectories at three different heights (500 m, 1000 m, 1500 m) every 8 h to provide information on the air parcel origins (Figure 4a). The air mass trajectories could be classified into four sectors: Sector A: Japan, yellow sea and bohai; Sector B: Southeast of China, the Pacific Ocean; Sector C: Southwest of Jiangsu and Anhui province; Sector D: Northern Asia inland and Mongolia region.

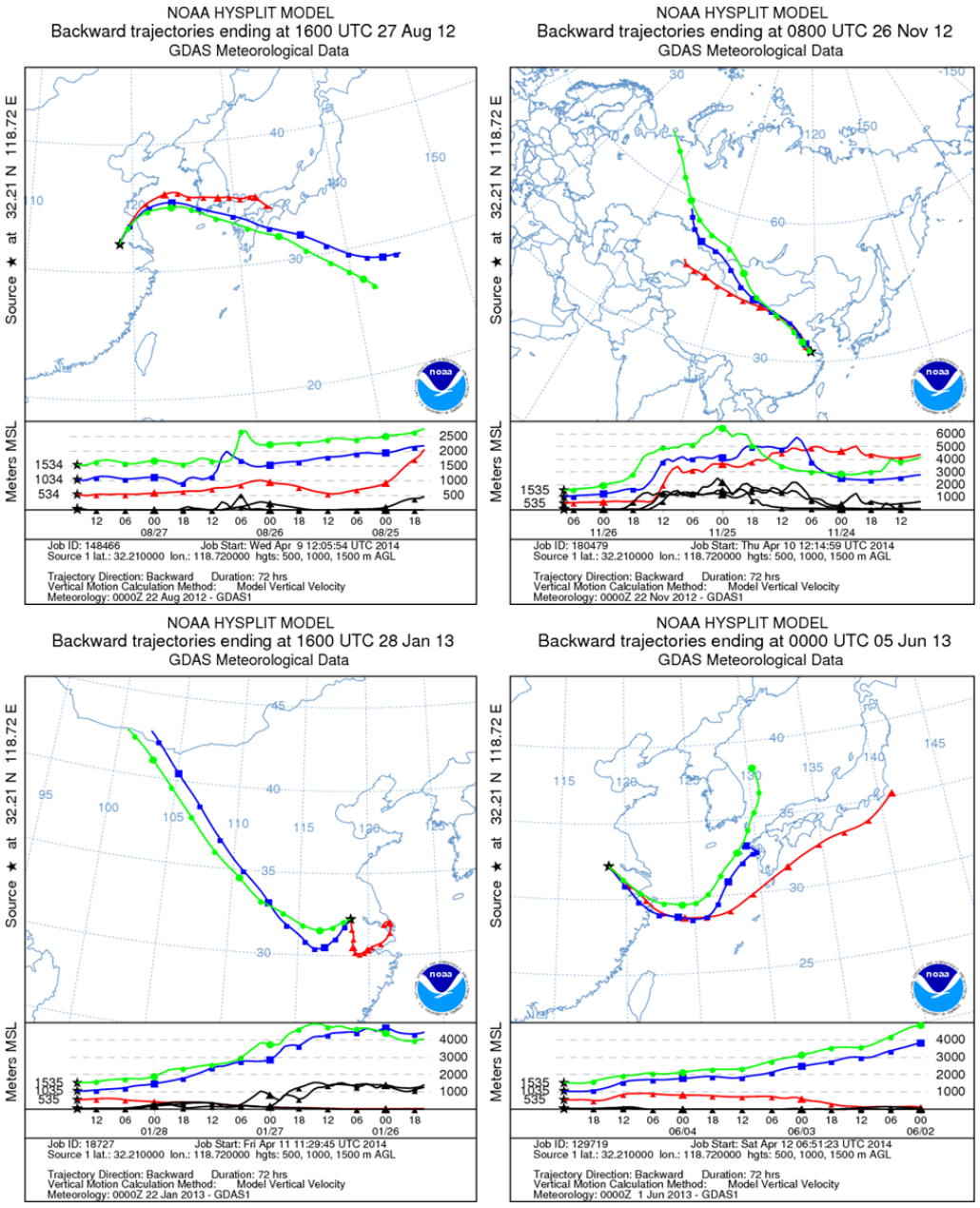

(**a**)

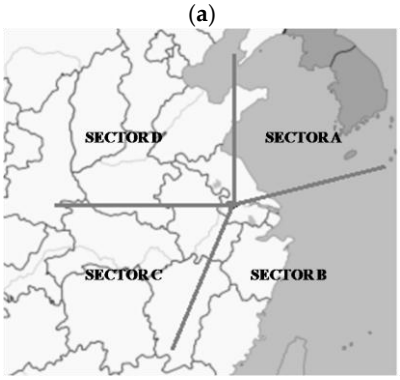

(**b**)

Figure 4. Hybrid Single-Particle Lagrangian Intgrated Trajectory (HYSPLIT) back trajectories showing the paths of the aerosol parcel during the sampling period; (**a**) back trajectories in four seasons; (**b**) Air parcel trajectory sectors.

In summer, the air parcels mainly came from the ocean, including Sectors A and B, except for 28 August from Anhui province (Sector C), and 29 August, 30 August, 5 September and 8 September from the north of China (Sector D). The air masses during these special days (Figure 2) can be traced back to NW of Mongolia. Since this trajectory intercepts with numerous industrial and suburban areas of northern China, which delivered polluted air to the receptor site, the concentrations of metal elements in Figure 3, like Mn, Pb, Ba, Cd, Ni, Sr, V, showed peak values in summer. The back trajectories in autumn and winter indicate three air mass pathways: Sector B, Sector C and more predominantly Sector D. It has been mentioned earlier that some elements had higher values in these two seasons, probably because of the air parcels from North of China, which not only transport the cold air but also the pollutants, such as heating-related or coal burning emissions during these cold seasons. This influence can be observed in Figure 3 by the characteristics of elements like As, Sb and Sr. Cu had a peak concentration on 18 and 19 November in autumn, similar to Mg, Mn, Pb, which is likely due to two reasons: (1) the wind mostly blew form the North in these two days, thus leading to high loadings of aerosol metals; (2) in the next two days, the wind direction changed to the NE, and the air parcel came from the ocean (Figure 4a), which carried clean air and led to the sudden decrease of the concentrations of these metals. In spring, Sector B was the main origin of air parcels, with the air coming only from the NW in May 28. On the other hand, as our sampling location resided in the suburban area and was adjacent to the farmland, the aerosol characteristics were inevitably influenced by local biomass burning emissions which released metal elements such as As, Cd, etc., into the atmosphere.

3.2. Source Apportionment of Selected Atmospheric Metal Elements

In this study, 64 samples with 17 metal species were inputted into the PMF 3.0 model. The PMF algorithm is able to segregate the total airborne metals into the sum of a few dominant sources, and quantify the temporal variations and contributions of each source [46,63]. In general, inclusion of more samples (>100 samples) can provide better PMF results and more scientifically sound interpretation of the sources. Nevertheless, applications of PMF model on a limited number of samples were also reported previously, and can also provide very valuable insights into the sources and processes of the aerosols. For example, [64] analyzed about in 57 samples from four cities, and identified different sources during heavy haze formation in China; [65] analyzed in total 24 samples from four sites to elucidate the sources and transformation processes of the water-soluble organic aerosols. In this study, the PMF results were carefully evaluated by investigating the characteristics of different solution spaces, for examples, five-, six- and seven-factor solutions. However, the five- and seven-factor solutions appeared to be physically unreasonable, and six sources were determined as the optimal solution, with the $f$peak of -0.1, the Qrobust and Qtrue values being almost equal to the Qtheory. The six factors were physically reasonable and also consistent with the potential aerosol sources in Nanjing (United States Environmental Protection Agency US EPA 2008). The profiles and corresponding time series of the six sources are shown in Figures 5 and 6, respectively.

Factor 1 contains high contributions of Pb (45.62%), Mn (43.33%), V (41.44%), Cu (38.38%), Se (38.88%), Mg (34.08%), Zn (33.40%), Cd (30.39%), and Ni (29.56%), indicating a predominant traffic source. Tire abrasion and brake wearing can generate debris particles that contain significant amounts of Zn, Cd, Pb, and Cu [34,66,67]. Vehicular exhaust emissions may contain V, Ni, Zn, Pb, and Se from gasoline, oil or fuel additives [68]. Seasonal variations shown in Figure 6 indicate that the traffic-related metal concentrations were higher in summer and spring, and lower in colder seasons (i.e., winter). This trend could be related to increased advection from upwind urban sites [23].

Factor 2 corresponds to soil/dust source as it contains the highest concentrations of a key crustal element—Al (82.88%) mixed with Na (17.61%) and Mg (16.47%). The soil dust could be contributed by fly ash from industrial activities nearby or other regions, or re-suspended dust due to traffic or construction activities. According to the time series of soil dust contribution (Figure 6), there was a sharp rise in summer; but the air parcels came from the Sector A (Figure 4b), the wind direction

was NE and the wind speed was low enough, so this bump may have resulted from the behaviors of anthropogenic emissions around the sampling site.

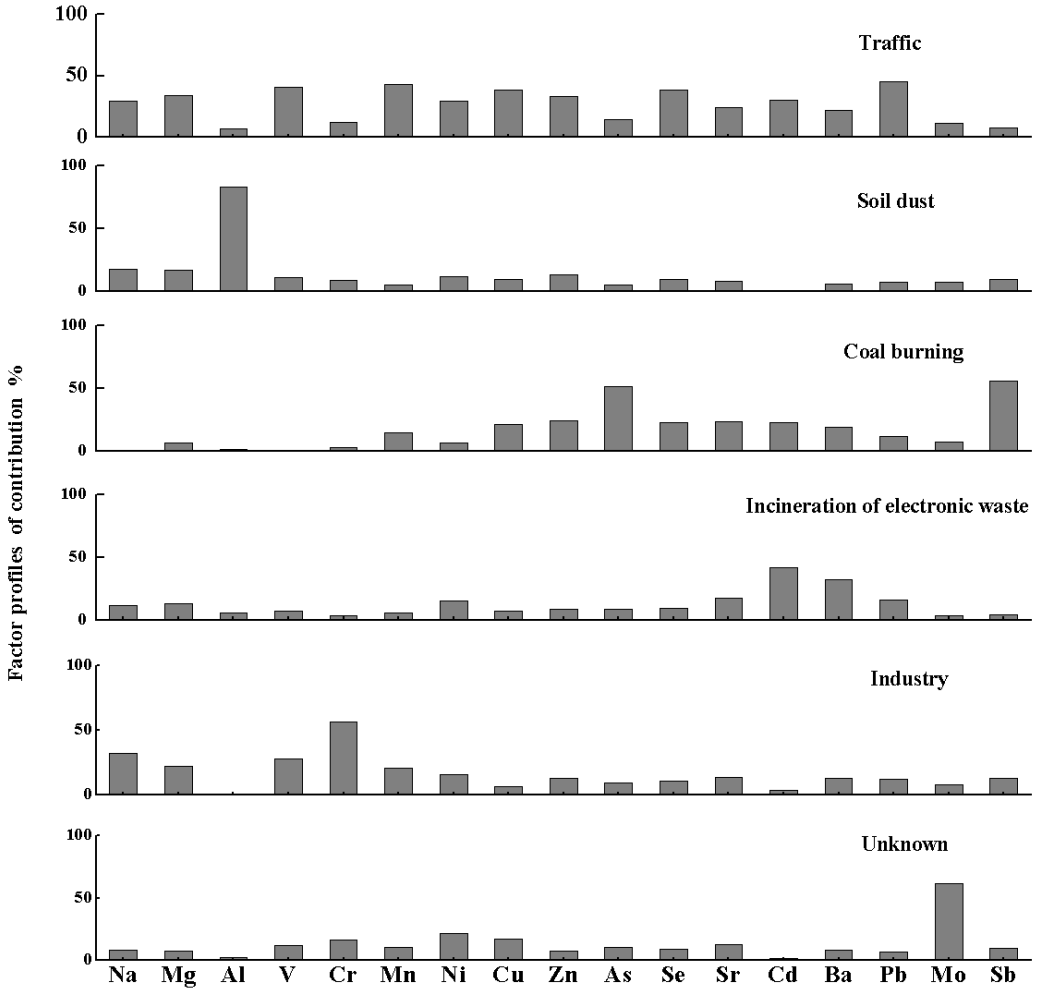

Figure 5. Contributions of metal elements to each sources (% of species total) analyzed by EPA positive matrix factorization (PMF).

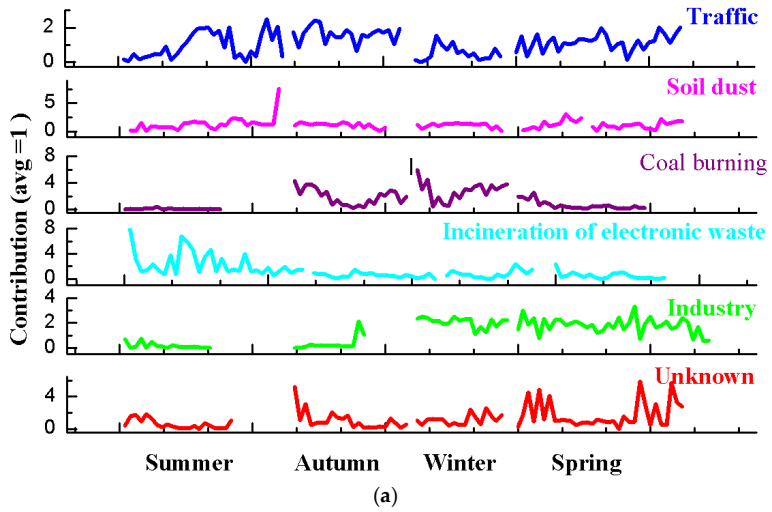

Figure 6. *Cont.*

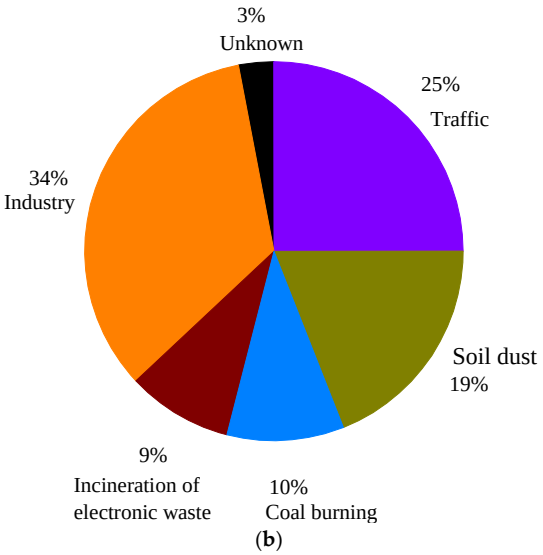

Figure 6. (**a**) Source contributions deduced from the PMF analysis of $PM_{2.5}$; (**b**) Pie of the contributions.

Factor 3 was identified as coal burning, as it contains high fractions of the heavy metals, including Sb (56.21%), As (51.63%), Zn (24.65%), Sr (24.06%), Se (23.15%), and Cd (23.10%). Sb, Se and Sr are commonly used as markers of coal burning emissions [29]. In addition to coal burning, As can be also emitted by iron making and steelmaking processes [69]. As shown in Figure 6, the contributions of coal burning factor were significantly high in autumn (31.49%) and winter (35.07%), in accordance with the enhanced coal consumption for energy supply during the cold seasons. Furthermore, during autumn and winter, the wind and air parcels (Figures 2 and 5a) were mainly derived from north China where coal burning is very active. It also should be mentioned that a large iron and steel plant is only a few kilometers away from our sampling site, and coal burning is a primary energy source for iron and steel production. A previous report (Yang et al. [63]) showed that in Beijing, coal burning from coal power plants, iron and steel industries contributed to 25% of the emitted $PM_{2.5}$ mass.

Factor 4 with markedly high contributions from elements like Cd (41.48%), Ba (32.06%), and relatively high contributions from Sr (17%), Pb (16.17%), and Ni (15.06%), likely represents the source of incineration of electronic waste. Earlier studies identified a variety of electronic materials, including batteries (Ni-Cd, Pb batteries), electric switches, electronic components of TV which contain Cadmium compounds [70,71], so incineration of these different types of electronic wastes can emitted metal-containing particles. Furthermore, this incineration is also associated with elements of Ba, Ni, Pb, Sr, which were usually used to produce the electric products like light bulb, TV tube or computer and so on [72]. Figure 6 showed the seasonal trend of this factor—the peak occurred in summer, likely due to enhanced applications of various electronic devices during summer.

Factor 5 was characterized by high percentages of Cr (56.38%), Na (32.35%), V (27.84%), Mn (20.41%), and Ni (15.87%). These elements were strongly associated with the industrial emissions in the vicinity of our site, especially for Cr and V [39,73]. Combustion of fossil fuels or oil burning can emit particles containing Cr, V, and Ni, and those activities often occur in the petrochemical and chemical plants [74]. Also, iron and steel production is likely an important source of Mn and Ni. Note that our sampling site is located at a region close to many industrial plants and thus may experience serious industrial pollutants. The seasonal variations were (Figure 6) showed that industry contributed more significantly in winter and spring than in other seasons, which might be attributed to the low mixing layer height and stagnant wind conditions, resulting in the accumulation of the industry-related metal-containing particles near our sampling site.

Factor 6 (Unknown) was a main contributor to Mo (61.93%), Ni (21.43%), Cu (17.08%) in ambient $PM_{2.5}$. In previous studies, Mo was identified as a tracer of a hard alloy plant which produces molybdenum

alloy and Ni [75]. Mo was also observed in particles from diesel emissions (Duan and Tan [39]); however, this source needs further investigation. Factor 6 had a high contribution only in spring.

Overall, the contributions of different sources to the total aerosol metals were factor 5 (Industry, 34%), factor 1 (Traffic, 25%), factor 2 (Soil dust, 19%), factor 3 (coal burning, 10%), factor 4 (Incineration of electronic waste, 9%), and factor 6 (Unknown, 3%).

3.3. Particle Morphology and Composition

SEM technique was used to analyze the particle morphology [76,77], and EDS analysis was applied to provide the elemental composition of aerosol particles quantitatively (Figure 7), so as to aid the source apportionment analyses.

Our SEM measurements identified three major types of morphology of the sampled particles. The first type appears to be mineral grains with the typical shape of single or aggregated regular columnar crystal (Figure 7a). EDS showed that these particles contain mainly silicon aluminate, quartz, calcium, iron and a small amount of other metal elements. For example, EDS analyses that identified the elemental compositions of a typical mineral grain were Ca, S and O, indicating the presence of gypsum ($CaSO_4 \cdot H_2O$) [9,78] The gypsum particles could be traced to several sources, such as secondary reactions involving SO_2, airborne limestone, photocatalytical conversion by Fe_2O_3 or TiO_2 of dust-related species, or directly from coal combustion [79] and desulfurization. Fe mainly came from industries; and Ti or K may be associated with crustal particles. Although previous studies indicated that mineral particles may generate from construction activities [31,79], it has been demonstrated that the morphology of such particles is typically porous, therefore the gypsum particles observed in this study are unlikely from construction source. The second type of particles are spherical with a smooth surface by the SEM (Figure 7b), and EDS further showed that they were predominately alumino-silicates classified as fly ash, supporting that these particles were mainly derived from coal combustion and metallurgical processes. Another type of spherical particles (Figure 7c) was mainly composed of C and O and thus likely consisted of organics. Overall, the qualitative analyses by the SEM/EDS results indicated the particle sources of coal burning, industrial emissions and soil dust, which is consistent with the PMF results.

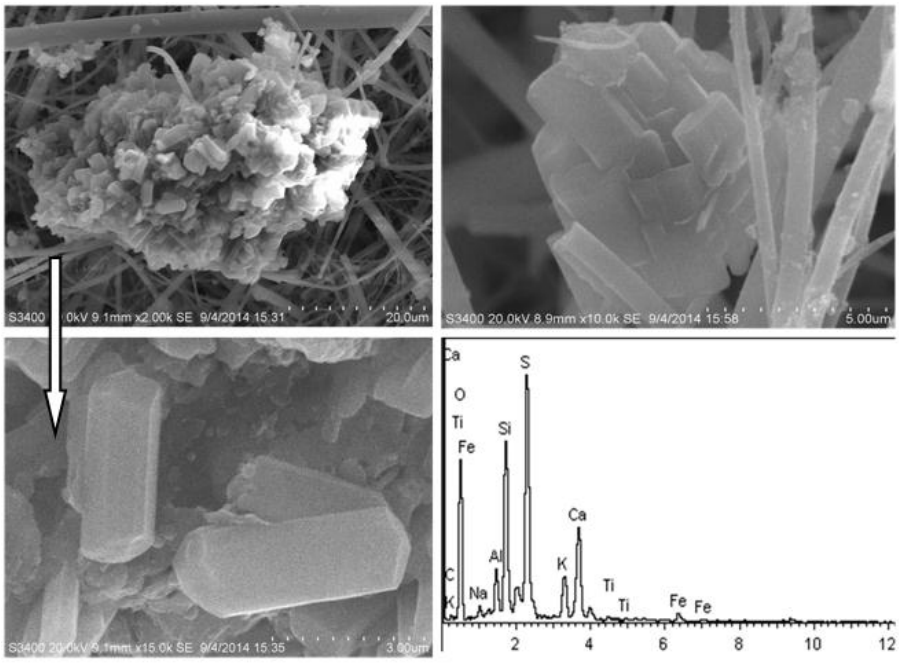

(**a**)

Figure 7. *Cont.*

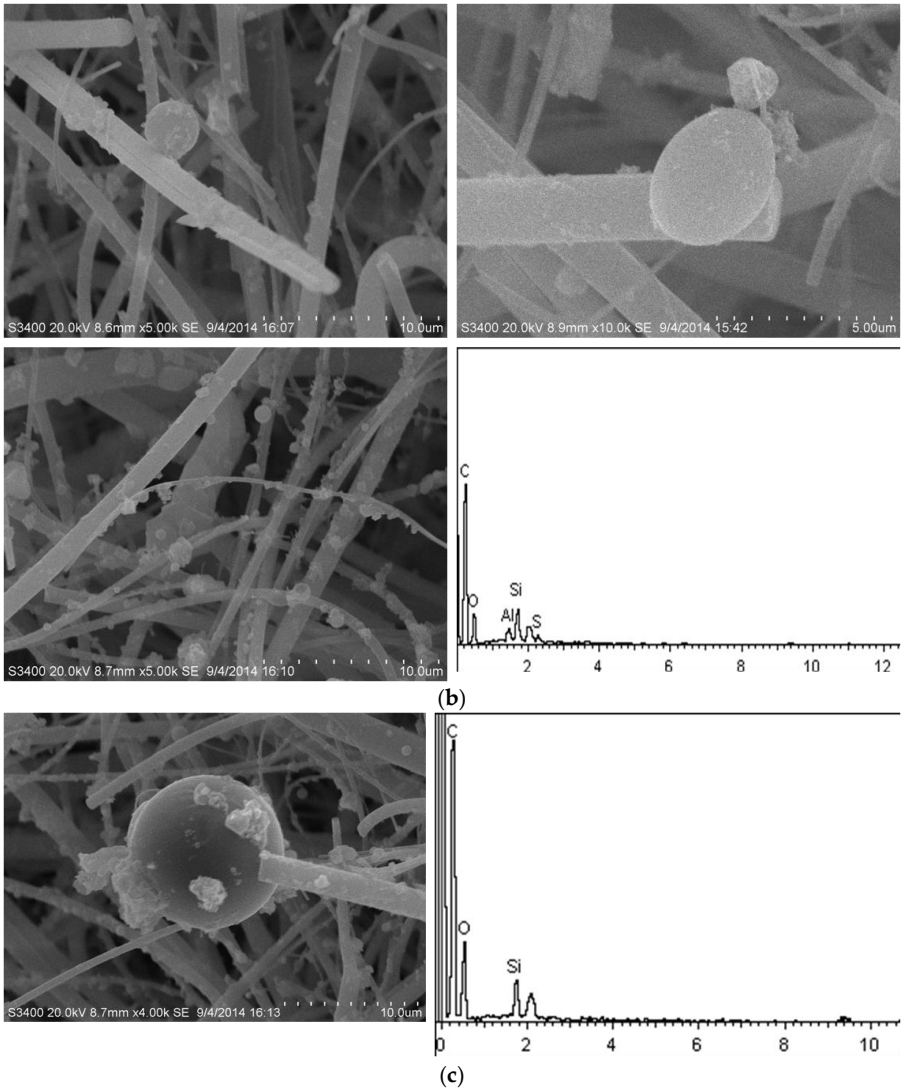

Figure 7. SEM/EDS photomicrographs of (**a**) mineral particles; (**b**) fly ash, quartz particles; (**c**) carbon particles.

4. Conclusions

This study presents measurement results of 17 metal elements in $PM_{2.5}$ samples collected over a one-year period. Chemical characteristics including concentrations, temporal variations, sources, morphology, and air mass trajectories were thoroughly discussed. We found that the airborne metal mass loadings in suburban Nanjing was on average, 1.23 $\mu g/m^3$, accounting for 1.0% of the total $PM_{2.5}$ mass, which is comparable with those observed in other polluted cities in China. In particular, we found that the element of As concentrations was above the reference values of NAQQS (GB3095-2012) and WHO guidelines. Temporal changes of these metals behaved differently due to variations of emission sources, air mass origins, and meteorological conditions. Across the sampling period, we identified and quantified six major sources for the observed metal elements, including industry (34%), traffic (25%), soil dust (19%), coal burning (10%), incineration of electronic waste (9%), and a minor unknown source (3%). Further SEM/EDS analyses of the particles verified the source apportionment results. As the heavy metals have multiple adverse effects on the environment and public health, our findings are thus valuable for the air quality remediation in the densely populated YRD region, and may provide insights for evaluating the environmental influences of metals on soil, water and the ecosystem.

Supplementary Materials: The following are available online at www.mdpi.com/2073-4433/7/12/153/s1, Figure S1: The comparison of wind direction and wind speed between four seasons and collecting days. (a–d) shows the WD and WS in different seasons (data of per hour); (e–h) shows the WD and WS in the collecting days, Figure S2: The comparison of diurnal variation of Temperature, Relative humidity, Wind speed between whole the summer (data of per hour) and collection days in summer, Figure S3: The comparison of diurnal variation of Temperature, Relative humidity, Wind speed between whole the autumn (data of per hour) and collection days in autumn, Figure S4: The comparison of diurnal variation of Temperature, Relative humidity, Wind speed between whole the winter (data of per hour) and collection days in winter, Figure S5: The comparison of diurnal variation of Temperature, Relative humidity, Wind speed between whole the spring (data of per hour) and collection days in spring, Table S1: The date of sixty-four samples, Table S2: The recovery of the two certified materials of soil (GBW07403) and fly ash (GBW08401) (n = 10).

Acknowledgments: This work was supported by Commonweal Program of Environment Protection Department of China (Grant No. 201409027-05); International ST Cooperation Program of China (ISTCP) (Grant No. 2014DFA90780); National Natural Science Foundation of China (21407079, 21577065); A significant Research Plan of National Natural Science Foundation of China (91543115); and the Priority Academic Program Development of Jiangsu Higher Education Institutions.

Author Contributions: Mindong Chen, Xinlei Ge and Lu Qi conceived and designed the experiments; Yafei Zhang, Lu Qi and Bingfang Guo performed the experiments; Lu Qi wrote the paper. All the authors have read and approved the final manuscript.

Conflicts of Interest: The authors declare no conflict of interest.

References

1. Cohen, A. *Global Burden of Disease 2010*; Institute for Health Metrics and Evaluation: Washington, DC, USA, 2013.
2. Hu, X.; Zhang, Y.; Ding, Z.; Wang, T.; Lian, H.; Sun, Y.; Wu, J. Bioaccessibility and health risk of arsenic and heavy metals (Cd, Co, Cr, Cu, Ni, Pb, Zn and Mn) in TSP and $PM_{2.5}$ in Nanjing, China. *Atmos. Environ.* **2012**, *57*, 146–152. [CrossRef]
3. Ezzati, M.; Lopez, A.D.; Rodgers, A.; Vander Hoorn, S.; Murray, C.J.L. Selected major risk factors and global and regional burden of disease. *Lancet* **2002**, *360*, 1347–1360. [CrossRef]
4. Srivastava, A.; Jain, V.K. Size distribution and source identification of total suspended particulate matter and associated heavy metals in the urban atmosphere of Delhi. *Chemosphere* **2007**, *68*, 579–589. [CrossRef] [PubMed]
5. Zhang, Y.; Obrist, D.; Zielinska, B.; Gertler, A. Particulate emissions from different types of biomass burning. *Atmos. Environ.* **2013**, *72*, 27–35. [CrossRef]
6. Schwarz, J.; Stefancova, L.; Maenhaut, W.; Smolik, J.; Zdimal, V. Mass and chemically speciated size distribution of Prague aerosol using an aerosol dryer–the influence of air mass origin. *Sci. Total Environ.* **2012**, *437*, 348–362. [CrossRef] [PubMed]
7. Lopez, A.D.; Mathers, C.D.; Ezzati, M.; Jamison, D.T.; Murray, C.J. Measuring the global burden of disease and risk factors, 1990–2001. *Glob. Burd. Dis. Risk Factors* **2006**, *1*, 1–14.
8. Zhang, J.J.; Smith, K.R. Household air pollution from coal and biomass fuels in China: Measurements, health impacts, and interventions. *Environ. Health Perspect.* **2007**, *115*, 848–855. [CrossRef] [PubMed]
9. Allen, A.G.; Nemitz, E.; Shi, J.P.; Harrison, R.M.; Greenwood, J.C. Size distributions of trace metals in atmospheric aerosols in the United Kingdom. *Atmos. Environ.* **2001**, *35*, 4581–4591. [CrossRef]
10. Moreno, T.; Kojima, T.; Querol, X.; Alastuey, A.; Amato, F.; Gibbons, W. Natural versus anthropogenic inhalable aerosol chemistry of transboundary East Asian atmospheric outflows into western Japan. *Sci. Total Environ.* **2012**, *424*, 182–192. [CrossRef] [PubMed]
11. Soriano, A.; Pallarés, S.; Pardo, F.; Vicente, A.B.; Sanfeliu, T.; Bech, J. Deposition of heavy metals from particulate settleable matter in soils of an industrialised area. *J. Geochem. Explor.* **2012**, *113*, 36–44. [CrossRef]
12. Pereira, P.A.P.; Lopes, W.A.; Carvalho, L.S.; da Rocha, G.O.; Nei de Bahia, C.; Loyola, J.; Quiterio, S.L.; Escaleira, V.; Arbilla, G.; de Andrade, J.B. Atmospheric concentrations and dry deposition fluxes of particulate trace metals in Salvador, Bahia, Brazil. *Atmos. Environ.* **2007**, *41*, 7837–7850. [CrossRef]
13. Jalkanen, L.; Makinen, A.; Hasanen, E.; Juhanoja, J. The effect of large anthropogenic particulate emissions on atmospheric aerosols, deposition and bioindicators in the eastern Gulf of Finland region. *Sci. Total Environ.* **2000**, *262*, 123–136. [CrossRef]

14. Connan, O.; Maro, D.; Hébert, D.; Roupsard, P.; Goujon, R.; Letellier, B.; Cavelier, S.L. Wet and dry deposition of particles associated metals (Cd, Pb, Zn, Ni, Hg) in a rural wetland site, Marais Vernier, France. *Atmos. Environ.* **2012**, *67*, 394–403. [CrossRef]
15. Seinfeld, J.H.; Pandis, S.N. *Atmospheric Chemistry and Physics: From Air Pollution to Climate Change*; Wiley: Hoboken, NJ, USA, 2012.
16. Yi, S.-M.; Totten, L.A.; Thota, S.; Yan, S.; Offenberg, J.H.; Eisenreich, S.J.; Graney, J.; Holsen, T.M. Atmospheric dry deposition of trace elements measured around the urban and industrially impacted NY–NJ harbor. *Atmos. Environ.* **2006**, *40*, 6626–6637. [CrossRef]
17. Ahiablame, L.M.; Engel, B.A.; Chaubey, I. Effectiveness of low impact development practices: Literature review and suggestions for future research. *Water Air Soil Pollut.* **2012**, *223*, 4253–4273. [CrossRef]
18. Solomon, S. *Climate Change 2007-The Physical Science Basis: Working Group I Contribution to the Fourth Assessment Report of the IPCC*; Cambridge University Press: Cambridge, UK, 2007.
19. Valavanidis, A.; Fiotakis, K.; Bakeas, E.; Vlahogianni, T. Electron paramagnetic resonance study of the generation of reactive oxygen species catalysed by transition metals and quinoid redox cycling by inhalable ambient particulate matter. *Redox Rep.* **2005**, *10*, 37–51. [CrossRef] [PubMed]
20. Seaton, E.K.; Caldwell, C.H.; Sellers, R.M.; Jackson, J.S. An intersectional approach for understanding perceived discrimination and psychological well-being among African American and Caribbean Black youth. *Dev. Psychol.* **2010**, *46*, 1372. [CrossRef] [PubMed]
21. Laden, F.; Neas, L.M.; Dockery, D.W.; Schwartz, J. Association of fine particulate matter from different sources with daily mortality in six US cities. *Environ. Health Perspect.* **2000**, *108*, 941–947. [CrossRef] [PubMed]
22. Schmeling, M. Seasonal variations in diurnal concentrations of trace elements in atmospheric aerosols in Chicago. *Anal. Chim. Acta* **2003**, *496*, 315–323. [CrossRef]
23. Saffari, A.; Daher, N.; Shafer, M.M.; Schauer, J.J.; Sioutas, C. Seasonal and spatial variation of trace elements and metals in quasi-ultrafine (PM0.25) particles in the Los Angeles metropolitan area and characterization of their sources. *Environ. Pollut.* **2013**, *181*, 14–23. [CrossRef] [PubMed]
24. Brown, R.J.; Yardley, R.E.; Muhunthan, D.; Butterfield, D.M.; Williams, M.; Woods, P.T.; Brown, A.S.; Goddard, S.L. Twenty-five years of nationwide ambient metals measurement in the United Kingdom: Concentration levels and trends. *Environ. Monit. Assess.* **2008**, *142*, 127–140. [CrossRef] [PubMed]
25. Heimbürger, L.-E.; Migon, C.; Dufour, A.; Chiffoleau, J.-F.; Cossa, D. Trace metal concentrations in the North-western Mediterranean atmospheric aerosol between 1986 and 2008: Seasonal patterns and decadal trends. *Sci. Total Environ.* **2010**, *408*, 2629–2638. [CrossRef] [PubMed]
26. Pulles, T.; Gon, H.D.; Appelman, W.; Verheul, M. Emission factors for heavy metals from diesel and petrol used in European vehicles. *Atmos. Environ.* **2012**, *61*, 641–651. [CrossRef]
27. Ilyin, I.; Rozovskaya, O.; Travnikov, O.; Varygina, M.; Aas, W.; Uggerud, H. *Heavy Metals: Transboundary Pollution of the Environment, EMEP Status Report 2/2011*; Norwegian Institute for Air Research, Kjeller, Norway and Meteorological Synthesizing Centre-East: Moscow, Russia, 2011.
28. Makkonen, U.; Hellen, H.; Anttila, P.; Ferm, M. Size distribution and chemical composition of airborne particles in south-eastern Finland during different seasons and wildfire episodes in 2006. *Sci. Total Environ.* **2010**, *408*, 644–651. [CrossRef] [PubMed]
29. Pan, Y.; Wang, Y.; Sun, Y.; Tian, S.; Cheng, M. Size-resolved aerosol trace elements at a rural mountainous site in Northern China: Importance of regional transport. *Sci. Total Environ.* **2013**, *461–462*, 761–771. [CrossRef] [PubMed]
30. Duan, J.; Tan, J.; Hao, J.; Chai, F. Size distribution, characteristics and sources of heavy metals in haze episod in Beijing. *J. Environ. Sci.* **2014**, *26*, 189–196. [CrossRef]
31. Witt, M.L.I.; Meheran, N.; Mather, T.A.; de Hoog, J.C.M.; Pyle, D.M. Aerosol trace metals, particle morphology and total gaseous mercury in the atmosphere of Oxford, UK. *Atmos. Environ.* **2010**, *44*, 1524–1538. [CrossRef]
32. Mbengue, S.; Alleman, L.Y.; Flament, P. Size-distributed metallic elements in submicronic and ultrafine atmospheric particles from urban and industrial areas in northern France. *Atmos. Res.* **2014**, *135–136*, 35–47. [CrossRef]
33. Li, Z.; Feng, X.; Li, G.; Bi, X.; Zhu, J.; Qin, H.; Dai, Z.; Liu, J.; Li, Q.; Sun, G. Distributions, sources and pollution status of 17 trace metal/metalloids in the street dust of a heavily industrialized city of central China. *Environ. Pollut.* **2013**, *182*, 408–416. [CrossRef] [PubMed]

34. Song, F.; Gao, Y. Size distributions of trace elements associated with ambient particular matter in the affinity of a major highway in the New Jersey–New York metropolitan area. *Atmos. Environ.* **2011**, *45*, 6714–6723. [CrossRef]
35. Duan, J.; Tan, J.; Wang, S.; Hao, J.; Chai, F. Size distributions and sources of elements in particulate matter at curbside, urban and rural sites in Beijing. *J. Environ. Sci.* **2012**, *24*, 87–94. [CrossRef]
36. Keane, B.; Collier, M.H.; Shann, J.R.; Rogstad, S.H. Metal content of dandelion leaves in relation to soil contamination and airborne particulate matter. *Sci. Total Environ.* **2001**, *281*, 63–78. [CrossRef]
37. Pui, D.Y.H.; Chen, S.-C.; Zuo, Z. $PM_{2.5}$ in China: Measurements, sources, visibility and health effects, and mitigation. *Particuology* **2014**, *13*, 1–26. [CrossRef]
38. Rippey, B.; Rose, N.; Yang, H.; Harrad, S.; Robson, M.; Travers, S. An assessment of toxicity in profundal lake sediment due to deposition of heavy metals and persistent organic pollutants from the atmosphere. *Environ. Int.* **2008**, *34*, 345–356. [CrossRef] [PubMed]
39. Duan, J.; Tan, J. Atmospheric heavy metals and Arsenic in China: Situation, sources and control policies. *Atmos. Environ.* **2013**, *74*, 93–101. [CrossRef]
40. Mmari, A.G.; Potgieter-Vermaak, S.S.; Bencs, L.; McCrindle, R.I.; Van Grieken, R. Elemental and ionic components of atmospheric aerosols and associated gaseous pollutants in and near Dar es Salaam, Tanzania. *Atmos. Environ.* **2013**, *77*, 51–61. [CrossRef]
41. Pavuluri, C.M.; Kawamura, K.; Mihalopoulos, N.; Fu, P. Year-round observations of water-soluble ionic species and trace metals in Sapporo aerosols: Implication for significant contributions from terrestrial biological sources in Northeast Asia. *Atmos. Chem. Phys. Discuss.* **2013**, *13*, 6589–6629. [CrossRef]
42. Tan, J.-H.; Duan, J.-C.; Chen, D.-H.; Wang, X.-H.; Guo, S.-J.; Bi, X.-H.; Sheng, G.-Y.; He, K.-B.; Fu, J.-M.; El-Wahab, M. Chemical characteristics of haze during summer and winter in Guangzhou. *Atmos. Res.* **2009**, *94*, 238–245. [CrossRef]
43. Lee, C.S.L.; Li, X.-D.; Zhang, G.; Li, J.; Ding, A.-J.; Wang, T. Heavy metals and Pb isotopic composition of aerosols in urban and suburban areas of Hong Kong and Guangzhou, South China—Evidence of the long-range transport of air contaminants. *Atmos. Environ.* **2007**, *41*, 432–447. [CrossRef]
44. Cheng, S. Heavy metal pollution in China: Origin, pattern and control. *Environ. Sci. Pollut. Res.* **2003**, *10*, 192–198. [CrossRef]
45. Cao, Z.; Yang, Y.; Lu, J.; Zhang, C. Atmospheric particle characterization, distribution, and deposition in Xi'an, Shaanxi Province, Central China. *Environ. Pollut.* **2011**, *159*, 577–584. [CrossRef] [PubMed]
46. Richard, A.; Gianini, M.F.D.; Mohr, C.; Furger, M.; Bukowiecki, N.; Minguillón, M.C.; Lienemann, P.; Flechsig, U.; Appel, K.; DeCarlo, P.F.; et al. Source apportionment of size and time resolved trace elements and organic aerosols from an urban courtyard site in Switzerland. *Atmos. Chem. Phys.* **2011**, *11*, 8945–8963. [CrossRef]
47. Qi, L.; Zhang, Y.; Ma, Y.; Chen, M.; Ge, X.; Ma, Y.; Zheng, J.; Wang, Z.; Li, S. Source identification of trace elements in the atmosphere during the second Asian Youth Games in Nanjing, China: Influence of control measures on air quality. *Atmos. Pollut. Res.* **2016**, *7*, 547–556. [CrossRef]
48. Illuminati, S.; Bau, S.; Annibaldi, A.; Mantini, C.; Libani, G.; Truzzi, C.; Scarponi, G. Evolution of size-segregated aerosol mass concentration during the Antarctic summer at Northern Foothills, Victoria Land. *Atmos. Environ.* **2016**, *125*, 212–221. [CrossRef]
49. Illuminati, S.; Annibaldi, A.; Truzzi, C.; Libani, G.; Mantini, C.; Scarponi, G. Determination of water-soluble, acid-extractable and inert fractions of Cd, Pb and Cu in Antarctic aerosol by square wave anodic stripping voltammetry after sequential extraction and microwave digestion. *J. Electroanal. Chem.* **2015**, *755*, 182–196. [CrossRef]
50. Ramanathan, T.; Ting, Y.-P. Selection of wet digestion methods for metal quantification in hazardous solid wastes. *J. Environ. Chem. Eng.* **2015**, *3*, 1459–1467. [CrossRef]
51. Sánchez Vilas, J.; Campoy, J.G.; Retuerto, R. Sex and heavy metals: Study of sexual dimorphism in response to soil pollution. *Environ. Exp. Bot.* **2016**, *126*, 68–75. [CrossRef]
52. ICH Harmonized Tripartite Guideline, Validation of Analytical Procedure: Text and Methodologies, Q2 (R1). Available online: http://www.ich.org/fileadmin/Public_Web_Site/ICH_Products/Guidelines/Quality/Q2_R1/Step4/Q2_R1__Guideline.pdf (accessed on 23 November 2016).

53. Truzzi, C.; Illuminati, S.; Finale, C.; Annibaldi, A.; Lestingi, C.; Scarponi, G. Microwave-assisted solvent extraction of melamine from seafood and determination by gas chromatography–mass spectrometry: Optimization by factorial design. *Anal. Lett.* **2014**, *47*, 1118–1133. [CrossRef]
54. Truzzi, C.; Annibaldi, A.; Illuminati, S.; Finale, C.; Rossetti, M.; Scarponi, G. Determination of Very Low Levels of 5-(Hydroxymethyl)-2-furaldehyde (HMF) in Natural Honey: Comparison Between the HPLC Technique and the Spectrophotometric White Method. *J. Food Sci.* **2012**, *77*, C784–C790. [CrossRef] [PubMed]
55. Paatero, P. The multilinear engine—A table-driven, least squares program for solving multilinear problems, including the n-way parallel factor analysis model. *J. Comput. Graph. Stat.* **1999**, *8*, 854–888.
56. Paatero, P.; Tapper, U. Positive matrix factorization: A non-negative factor model with optimal utilization of error estimates of data values. *Environmetrics* **1994**, *5*, 111–126. [CrossRef]
57. Padoan, E.; Malandrino, M.; Giacomino, A.; Grosa, M.M.; Lollobrigida, F.; Martini, S.; Abollino, O. Spatial distribution and potential sources of trace elements in PM10 monitored in urban and rural sites of Piedmont Region. *Chemosphere* **2016**, *145*, 495–507. [CrossRef] [PubMed]
58. Zhou, S.; Yuan, Q.; Li, W.; Lu, Y.; Zhang, Y.; Wang, W. Trace metals in atmospheric fine particles in one industrial urban city: Spatial variations, sources, and health implications. *J. Environ. Sci.* **2014**, *26*, 205–213. [CrossRef]
59. Toscano, G.; Moret, I.; Gambaro, A.; Barbante, C.; Capodaglio, G. Distribution and seasonal variability of trace elements in atmospheric particulate in the Venice Lagoon. *Chemosphere* **2011**, *85*, 1518–1524. [CrossRef] [PubMed]
60. Chen, H.; Lu, X.; Li, L.Y.; Gao, T.; Chang, Y. Metal contamination in campus dust of Xi'an, China: A study based on multivariate statistics and spatial distribution. *Sci. Total Environ.* **2014**, *484*, 27–35. [CrossRef] [PubMed]
61. Chen, B.; Stein, A.F.; Maldonado, P.G.; Sanchez de la Campa, A.M.; Gonzalez-Castanedo, Y.; Castell, N.; de la Rosa, J.D. Size distribution and concentrations of heavy metals in atmospheric aerosols originating from industrial emissions as predicted by the HYSPLIT model. *Atmos. Environ.* **2013**, *71*, 234–244. [CrossRef]
62. Draxler, R.R.; Rolph, G. *HYSPLIT (HYbrid Single-Particle Lagrangian Integrated Trajectory) Model Access via NOAA ARL READY*; NOAA Air Resources Laboratory: Silver Spring, MD, USA, 2003.
63. Yang, L.; Cheng, S.; Wang, X.; Nie, W.; Xu, P.; Gao, X.; Yuan, C.; Wang, W. Source identification and health impact of $PM_{2.5}$ in a heavily polluted urban atmosphere in China. *Atmos. Environ.* **2013**, *75*, 265–269. [CrossRef]
64. Huang, R.J.; Zhang, Y.; Bozzetti, C.; Ho, K.F.; Cao, J.J.; Han, Y.; Daellenbach, K.R.; Slowik, J.G.; Platt, S.M.; Canonaco, F.; et al. High secondary aerosol contribution to particulate pollution during haze events in China. *Nature* **2014**, *514*, 218–222. [CrossRef] [PubMed]
65. Sun, Y.; Zhang, Q.; Zheng, M.; Ding, X.; Edgerton, E.S.; Wang, X. Characterization and source apportionment of water-soluble organic matter in atmospheric fine particles ($PM_{2.5}$) with high-resolution aerosol mass spectrometry and GC-MS. *Environ. Sci. Technol.* **2011**, *45*, 4854–4861. [CrossRef] [PubMed]
66. Young, T.M.; Heeraman, D.A.; Sirin, G.; Ashbaugh, L.L. Resuspension of soil as a source of airborne lead near industrial facilities and highways. *Environ. Sci. Technol.* **2002**, *36*, 2484–2490. [CrossRef] [PubMed]
67. Bukowiecki, N.; Lienemann, P.; Hill, M.; Figi, R.; Richard, A.; Furger, M.; Rickers, K.; Falkenberg, G.; Zhao, Y.; Cliff, S.S. Real-world emission factors for antimony and other brake wear related trace elements: Size-segregated values for light and heavy duty vehicles. *Environ. Sci. Technol.* **2009**, *43*, 8072–8078. [CrossRef] [PubMed]
68. Harrison, R.M.; Tilling, R.; Callén Romero, M.A.S.; Harrad, S.; Jarvis, K. A study of trace metals and polycyclic aromatic hydrocarbons in the roadside environment. *Atmos. Environ.* **2003**, *37*, 2391–2402. [CrossRef]
69. Tian, H.; Wang, Y.; Xue, Z.; Cheng, K.; Qu, Y.; Chai, F.; Hao, J. Trend and characteristics of atmospheric emissions of Hg, As, and Se from coal combustion in China, 1980–2007. *Atmos. Chem. Phys.* **2010**, *10*, 11905–11919. [CrossRef]
70. Deng, W.J.; Louie, P.K.K.; Liu, W.K.; Bi, X.H.; Fu, J.M.; Wong, M.H. Atmospheric levels and cytotoxicity of PAHs and heavy metals in TSP and $PM_{2.5}$ at an electronic waste recycling site in southeast China. *Atmos. Environ.* **2006**, *40*, 6945–6955. [CrossRef]
71. Fang, G.; Wu, Y.; Huang, S.; Rau, J. Review of atmospheric metallic elements in Asia during 2000–2004. *Atmos. Environ.* **2005**, *39*, 3003–3013. [CrossRef]

72. Shah, M.H.; Shaheen, N. Seasonal behaviours in elemental composition of atmospheric aerosols collected in Islamabad, Pakistan. *Atmos. Res.* **2010**, *95*, 210–223. [CrossRef]
73. Zheng, Y.; Teng, Y. Emission characteristics of vanadium in air. *Environ. Sci. Manag.* **2012**, *37*, 20–24.
74. Kara, M.; Dumanoglu, Y.; Altiok, H.; Elbir, T.; Odabasi, M.; Bayram, A. Seasonal and spatial variations of atmospheric trace elemental deposition in the Aliaga industrial region, Turkey. *Atmos. Res.* **2014**, *149*, 204–216. [CrossRef]
75. Tao, J.; Gao, J.; Zhang, L.; Zhang, R.; Che, H.; Zhang, Z.; Lin, Z.; Jing, J.; Cao, J.; Hsu, S.C. $PM_{2.5}$ pollution in a megacity of southwest China: Source apportionment and implication. *Atmos. Chem. Phys. Discuss.* **2014**, *14*, 5147–5196. [CrossRef]
76. Xiao, R.; Chen, X.; Wang, F.; Yu, G. The physicochemical properties of different biomass ashes at different ashing temperature. *Renew. Energy* **2011**, *36*, 244–249. [CrossRef]
77. Lü, S.; Zhang, R.; Yao, Z.; Yi, F.; Ren, J.; Wu, M.; Feng, M.; Wang, Q. Size distribution of chemical elements and their source apportionment in ambient coarse, fine, and ultrafine particles in Shanghai urban summer atmosphere. *J. Environ. Sci.* **2012**, *24*, 882–890. [CrossRef]
78. Senlin, L.; Zhenkun, Y.; Xiaohui, C.; Minghong, W.; Guoying, S.; Jiamo, F.; Paul, D. The relationship between physicochemical characterization and the potential toxicity of fine particulates ($PM_{2.5}$) in Shanghai atmosphere. *Atmos. Environ.* **2008**, *42*, 7205–7214. [CrossRef]
79. Xie, R.K.; Seip, H.M.; Leinum, J.R.; Winje, T.; Xiao, J.S. Chemical characterization of individual particles (PM10) from ambient air in Guiyang City, China. *Sci. Total Environ.* **2005**, *343*, 261–272. [CrossRef] [PubMed]